551·594·12

Metastable O^+ ions in Martian atmosphere

D. C. AGARWAL

J. K. Institute of Applied Physics and Technology, University of Allahabad, Allahabad

(Received 27 October 1969)

ABSTRACT. Production rates of atomic oxygen ions in the metastable states (^2P and ^2D) by photo-ionization have been calculated. Equilibrium distributions of these species have been calculated using recently measured rate-coefficients of ion-atom interchange and other ionic reactions. Finally, the zenith intensity of the (7318·6-7330A) multiplet of O+ in the dayglow has been calculated and found to be approximately in the range 4·5-8·0 R.

1. Introduction

For the ionospheric chemistry of the Martian atmosphere, metastable ions are of importance as they carry extra energy with them. Because of this extra energy, some reactions may occur which are not possible for the normal states. For instance, $O^+(^2D)$ ions may produce a simple charge exchange reaction $O^+ + CO_2 \rightarrow O + CO_2^+$ which is energetically possible.

In this paper, metastable ions $O^+(^2P)$ and $O^+(^2D)$ in the day-time Martian atmosphere have been computed.

2. Models for the ionosphere of Mars

Three different models, namely, F_2, F_1 and E analogous to terrestrial ionosphere have been proposed by different investigators for the Martian ionosphere (Chamberlain and McElroy 1966; Donhaue 1966; McElroy 1967; Fjeldbo *et al.* 1968; and McElroy 1969). These models are shown in Figs. 1, 2 and 3 respectively. The density of respective neutral gas constituents are tabulated in Tables 1 to 3.

The critical question is the temperature distribution and photochemistry of CO_2 in Martian atmosphere. The temperature structure for these models are given in Fig. 4. It is evident from this figure that F_2 model requires a cold temperature profile which is not at all close to radiative balance and this cold profile is also not consistent with the measured amount of water vapour (Goody 1968). Further, the F_2 model gives no appreciable differences between temperature of electrons, ions and neutrals at this level, whereas detailed calculations and experience with earth's ionosphere suggest that pronounced differences should indeed exist. Because of these limitations, it is doubtful to follow the F_2 model of the Martian ionosphere.

The possibility of an F_1 layer is also ruled out because the number density required at 125 km are inconsistent with McElroy's (1967) radiative-diffusive equilibrium calculations by a quite wide margin.

Existence of an E layer seems to be favourable as it would not require a low temperature profile. But all E region theories encounter particular difficulties. If E layer does exist, the dissociative recombination of CO_2^+ must have a rate coefficient of 10^{-5} which is very high and a laboratory investigation is clearly indicated.

Thus an appropriate model of the Martian ionosphere is in doubt as yet. So, in the present calculations, we have calculated the equilibrium distributions of $O^+(^2P)$ and $O^+(^2D)$ ions for all the three models mentioned above.

3. Production rates

The photo-ionization reactions by which the metastable $O^+(^2P)$ and $O^+(^2D)$ ions may be produced are —

$$O(^3P) + P\ (\lambda \leqslant 663\ \text{A}) \rightarrow O^+(^2P) + e \qquad (1)$$

$$O(^3P) + P\ (\lambda \leqslant 732\ \text{A}) \rightarrow O^+(^2D) + e \qquad (2)$$

At an altitude z, the rate of production of the ions due to photo-ionization is given by—

$$q(\text{O})_{\lambda_z} = \gamma_\lambda\ n(P)_{\lambda_z}\ n(\text{O})_z \qquad (3)$$

where,

γ_λ = photo-ionization cross-section of O at the wavelength λ,

$n(P)_{\lambda_z}$ = photon flux density for the wavelength λ at the altitude z and

$n(\text{O})_z$ = concentration of O atoms at altitude z.

The productin rate of these ions for all wavelengths below the threshold is obtained by calculating the $q(\text{O})_{\lambda_z}$ at the small wavelength intervals of the

TABLE 1

F_2 Model of the Martian atmosphere

Altitude (km)	Temperature (°K)	$[CO_2]$ (cm^{-3})	$[CO]$ (cm^{-3})	$[O]$ (cm^{-3})
240	395	—	$4\cdot68\times10^{7}$	$8\cdot2\times10^{7}$
230	385	—	$5\cdot30\times10^{7}$	$1\cdot2\times10^{8}$
220	365	—	$6\cdot60\times10^{7}$	$3\cdot0\times10^{8}$
210	350	—	$8\cdot60\times10^{7}$	$7\cdot0\times10^{8}$
200	330	—	$1\cdot10\times10^{8}$	$9\cdot8\times10^{8}$
190	300	—	$1\cdot40\times10^{8}$	$1\cdot2\times10^{9}$
180	260	—	$1\cdot70\times10^{8}$	$2\cdot8\times10^{9}$
170	220	$3\cdot0\times10^{6}$	$2\cdot90\times10^{8}$	$5\cdot0\times10^{9}$
160	190	$6\cdot0\times10^{6}$	$3\cdot70\times10^{8}$	$8\cdot0\times10^{9}$
150	150	$1\cdot2\times10^{7}$	$4\cdot80\times10^{8}$	$1\cdot0\times10^{10}$
140	120	$3\cdot2\times10^{7}$	$6\cdot20\times10^{8}$	$2\cdot1\times10^{10}$
130	110	$4\cdot1\times10^{7}$	$7\cdot10\times10^{8}$	$3\cdot5\times10^{10}$
120	100	$4\cdot4\times10^{7}$	$1\cdot80\times10^{9}$	$5\cdot0\times10^{10}$
110	100	$2\cdot0\times10^{9}$	$4\cdot80\times10^{9}$	$7\cdot2\times10^{10}$
110	92	$3\cdot6\times10^{10}$	$1\cdot70\times10^{10}$	$8\cdot0\times10^{10}$
90	80	$3\cdot2\times10^{11}$	$4\cdot40\times10^{10}$	$9\cdot2\times10^{10}$
80	60	$2\cdot1\times10^{12}$	$9\cdot20\times10^{10}$	$1\cdot0\times10^{11}$
70	50	$1\cdot2\times10^{13}$	$4\cdot00\times10^{11}$	$4\cdot0\times10^{11}$
60	50	$6\cdot0\times10^{13}$	—	—
50	90	$2\cdot8\times10^{14}$	—	—
40	115	$2\cdot1\times10^{15}$	—	—
30	160	$4\cdot8\times10^{15}$	—	—
20	160	$1\cdot8\times10^{16}$	—	—
10	160	$5\cdot8\times10^{16}$	—	—
	160	$1\cdot7\times10^{17}$		

TALBE 2

F_1 Model of the Martian atmosphere

Altitude (km)	Temperature (°K)	$[CO_2]$ (cm^{-3})	$[CO]$ (cm^{-3})	$[O]$ (cm^{-3})
240	485	$3\cdot10\times10^{5}$	$2\cdot80\times10^{6}$	$9\cdot0\times10^{7}$
230	480	$1\cdot30\times10^{6}$	$6\cdot30\times10^{6}$	$1\cdot0\times10^{8}$
220	475	$3\cdot20\times10^{6}$	$1\cdot00\times10^{7}$	$1\cdot3\times10^{8}$
210	470	$8\cdot90\times10^{6}$	$1\cdot60\times10^{7}$	$1\cdot6\times10^{8}$
200	465	$2\cdot50\times10^{7}$	$2\cdot20\times10^{7}$	$2\cdot0\times10^{8}$
190	460	$9\cdot60\times10^{7}$	$4\cdot00\times10^{7}$	$2\cdot8\times10^{8}$
180	450	$2\cdot00\times10^{8}$	$8\cdot20\times10^{8}$	$4\cdot0\times10^{8}$
170	445	$7\cdot30\times10^{8}$	$1\cdot40\times10^{8}$	$6\cdot3\times10^{8}$
160	420	$1\cdot60\times10^{9}$	$2\cdot80\times10^{8}$	$1\cdot0\times10^{9}$
150	390	$4\cdot60\times10^{9}$	$6\cdot10\times10^{8}$	$1\cdot6\times10^{9}$
140	350	$1\cdot60\times10^{10}$	$1\cdot30\times10^{9}$	$2\cdot9\times10^{9}$
130	300	5.00×10^{10}	$2\cdot60\times10^{9}$	$5\cdot0\times10^{9}$
120	270	$1\cdot70\times10^{11}$	$6\cdot30\times10^{9}$	$8\cdot0\times10^{9}$
110	230	$6\cdot30\times10^{11}$	$1\cdot40\times10^{10}$	$1\cdot3\times10^{10}$
100	220	$2\cdot00\times10^{12}$	$3\cdot00\times10^{10}$	$3\cdot0\times10^{10}$
90	190	$7\cdot10\times10^{12}$	$7\cdot00\times10^{10}$	$7\cdot0\times10^{10}$*
80	160	$2\cdot80\times10^{13}$	$2\cdot00\times10^{11}$	$2\cdot2\times10^{11}$
70	150	$1\cdot00\times10^{14}$	$5\cdot00\times10^{11}$	$4\cdot0\times10^{11}$
60	130	$3\cdot20\times10^{14}$	—	—
50	120	$1\cdot00\times10^{15}$	—	—
40	125	$4\cdot00\times10^{15}$	—	—
30	130	$1\cdot00\times10^{16}$	—	—
20	140	$3\cdot20\times10^{16}$	—	—
10	150	$1\cdot00\times10^{17}$.	—	—
0	160	$2\cdot00\times10^{17}$	—	—

* The number density of (CO] and [O] have been extrapolated after 100 km

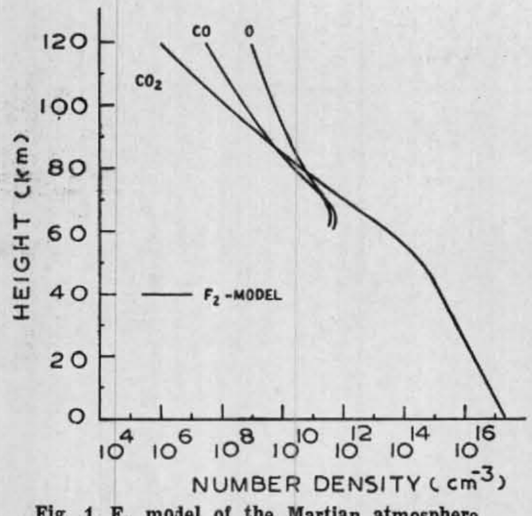

Fig. 1. F_2 model of the Martian atmosphere (Fjeldbo and Eshleman 1968)

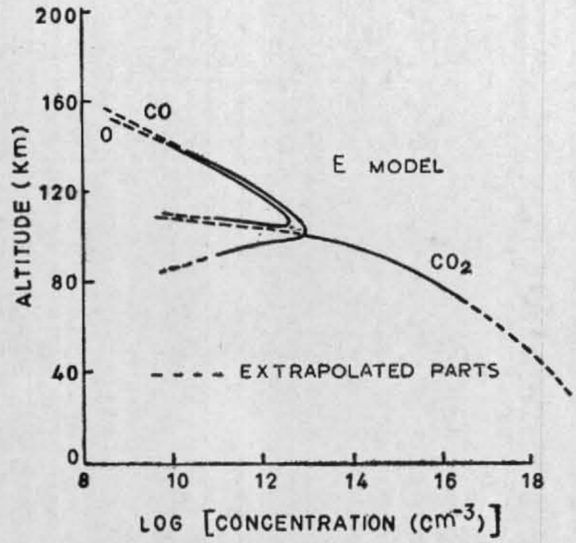

Fig. 3. E model of the Martian atmosphere (Chamberlain and McElroy 1966)

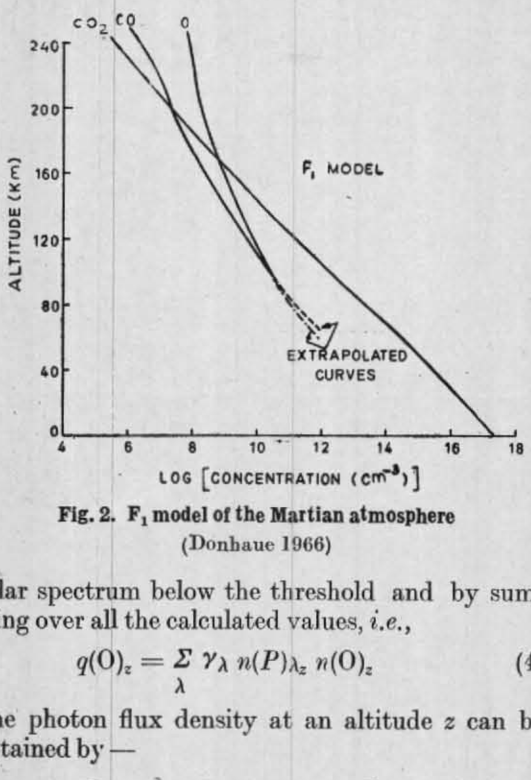

Fig. 2. F_1 model of the Martian atmosphere (Donhaue 1966)

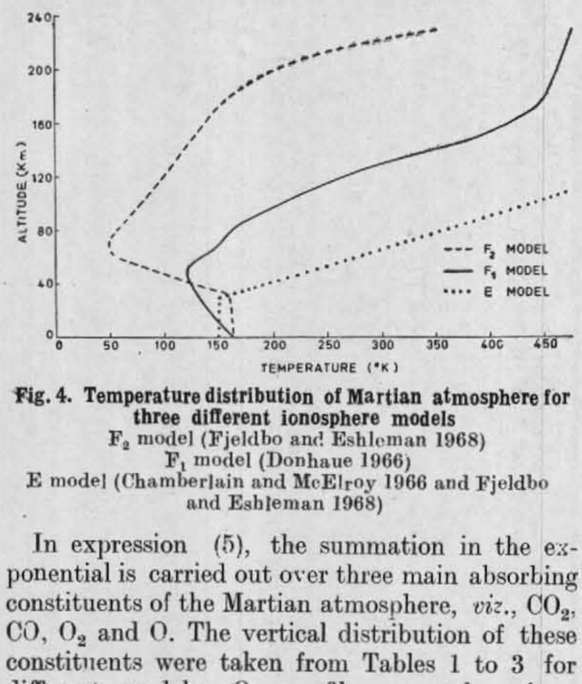

Fig. 4. Temperature distribution of Martian atmosphere for three different ionosphere models
F_2 model (Fjeldbo and Eshleman 1968)
F_1 model (Donhaue 1966)
E model (Chamberlain and McElroy 1966 and Fjeldbo and Eshleman 1968)

solar spectrum below the threshold and by summing over all the calculated values, *i.e.*,

$$q(\mathrm{O})_z = \sum_\lambda \gamma_\lambda \, n(P)_{\lambda_z} \, n(\mathrm{O})_z \quad (4)$$

The photon flux density at an altitude z can be obtained by —

$$n(P)_{\lambda_z} = n(P)_{\lambda_\infty} \exp\left[-\Sigma_i \, n_{i_z} \, H_{iz} \, \sigma_{i\lambda}\right] \quad (5)$$

where, $n(P)_{\lambda\infty}$ = photon flux density at the top of the atmosphere at the wavelength λ,

n_{i_z} = number density of i^{th} absorbing constituent at the altitude z,

H_{i_z} = scale height of i^{th} constituent at the altitude z and

$\sigma_{i\lambda}$ = absorption cross-section for i^{th} constituent at the wavelength λ.

In expression (5), the summation in the exponential is carried out over three main absorbing constituents of the Martian atmosphere, *viz.*, CO_2, CO, O_2 and O. The vertical distribution of these constituents were taken from Tables 1 to 3 for different models. O_2 profiles were taken from Chamberlain and McElroy's (1966) paper. Absorption cross-sections for CO_2 and CO were obtained from tabulations of Sun and Weissler (1957). For O_2 and O, the absorption cross-sections were taken from the data of Hinteregger *et al.* (1965). The photon flux density at different wavelengths were taken from the data of Hinteregger after multiplying each by 0·44, the dilution factor. The photon flux density at the top of the Martian atmosphere and photoionization cross-section of neutral particles used here are given in Table 4 as a function of wavelength band. The calculated rates of production for the two ionic species $O^+(^2P)$

TABLE 3

E Model of the Martian atmosphere

Altitude (km)	Temperature (°K)	$[CO_2]$ (cm^{-3})	$[CO]$ (cm^{-3})	$[O_2]$ (cm^{-3})	$[O]$ (cm^{-3})
120	500	—	$1\cdot0\times10^{12}$	—	$4\cdot1\times10^{12}$
110	470	$8\cdot0\times10^{11}$	$4\cdot2\times10^{12}$	$2\cdot1\times10^{11}$	$4\cdot1\times10^{12}$
100	430	$1\cdot8\times10^{13}$	$2\cdot0\times10^{13}$	$1\cdot0\times10^{12}$	$8\cdot1\times10^{11}$
90	390	$7\cdot0\times10^{14}$	$1\cdot0\times10^{13}$	$8\cdot0\times10^{11}$	$5\cdot3\times10^{10}$
80	350	$1\cdot0\times10^{15}$	$7\cdot0\times10^{12}$	$6\cdot5\times10^{10}$	$3\cdot2\times10^{9}$
70	310	$4\cdot0\times10^{15}$	$3\cdot1\times10^{12}$	$2\cdot1\times10^{8}$	$1\cdot6\times10^{8}$
60	270	$7\cdot0\times10^{15}$	$6\cdot2\times10^{11}$	$1\cdot0\times10^{6}$	$5\cdot7\times10^{7}$
50	230	$8\cdot5\times10^{15}$	—	—	—
40	190	$1\cdot0\times10^{16}$	—	—	—
30	150	$3\cdot5\times10^{16}$	—	—	—
20	150	$5\cdot1\times10^{16}$	—	—	—
10	150	$8\cdot3\times10^{16}$	—	—	—
0	150	$1\cdot4\times10^{17}$	—	—	—

TABLE 4

Photon flux density at the top of the Martian atmosphere and photo-ionization cross-section of CO_2, CO, O_2 and O at different wavelength bands

Wavelength Band ($\lambda\pm25$A°)	Photon flux density at the top of the Martian atmosphere [phontons cm^{-2} sec^{-1}(50A°)$^{-1}$]	Photo-ionization cross-section for O_2 (cm^2)	O (cm^2)	CO (cm^2)	CO_2 (cm^2)
50A	$0\cdot00456\times10^{10}$	$0\cdot165\times10^{-18}$	$0\cdot22\times10^{-18}$	$2\cdot1\times10^{-19}$	$3\cdot2\times10^{-19}$
100A	$0\cdot0152\times10^{10}$	$0\cdot66\times10^{-18}$	$0\cdot65\times10^{-18}$	$7\cdot5\times10^{-19}$	$1\cdot8\times10^{-18}$
150A	$0\cdot0269\times10^{10}$	$2\cdot60\times10^{-18}$	$1\cdot1\times10^{-18}$	$1\cdot15\times10^{-18}$	$4\cdot2\times10^{-18}$
200A	$0\cdot0556\times10^{10}$	$6\cdot82\times10^{-18}$	$3\cdot2\times10^{-18}$	$2\cdot61\times10^{-18}$	$1\cdot9\times10^{-17}$
250A	$0\cdot0724\times10^{10}$	$10\cdot5\times10^{-18}$	$5\cdot7\times10^{-18}$	$3\cdot6\times10^{-18}$	$2\cdot6\times10^{-17}$
300A	$0\cdot0465\times10^{10}$	$15\cdot7\times10^{-18}$	$8\cdot1\times10^{-18}$	$5\cdot0\times10^{-18}$	$1\cdot5\times10^{-17}$
350A	$0\cdot0189\times10^{10}$	$20\cdot3\times10^{-18}$	$8\cdot7\times10^{-18}$	$1\cdot0\times10^{-17}$	$2\cdot6\times10^{-17}$
400A	$0\cdot0216\times10^{10}$	$22\cdot5\times10^{-18}$	$10\cdot8\times10^{-18}$	$1\cdot5\times10^{-17}$	$2\cdot2\times10^{-17}$
450A	$0\cdot0243\times10^{10}$	$24\cdot1\times10^{-18}$	$11\cdot1\times10^{-18}$	$2\cdot0\times10^{-17}$	$2\cdot4\times10^{-17}$
500A	$0\cdot0303\times10^{10}$	$26\cdot5\times10^{-18}$	$12\cdot9\times10^{-18}$	$1\cdot9\times10^{-17}$	$2\cdot7\times10^{-17}$
550A	$0\cdot0357\times10^{10}$	$26\cdot5\times10^{-18}$	$13\cdot0\times10^{-18}$	$1\cdot9\times10^{-17}$	$2\cdot9\times10^{-17}$
600A	$0\cdot0390\times10^{10}$	$27\cdot6\times10^{-18}$	$13\cdot0\times10^{-18}$	$1\cdot8\times10^{-17}$	$3\cdot0\times10^{-17}$
650A	$0\cdot0422\times10^{10}$	$31\cdot6\times10^{-18}$	$11\cdot8\times10^{-18}$	$1\cdot7\times10^{-17}$	$2\cdot2\times10^{-17}$
700A	$0\cdot0456\times10^{10}$	$26\cdot2\times10^{-18}$	$8\cdot6\times10^{-18}$	$1\cdot6\times10^{-17}$	$1\cdot8\times10^{-17}$
750A	$0\cdot0487\times10^{10}$	$21\cdot4\times10^{-18}$	$5\cdot6\times10^{-18}$	$1\cdot3\times10^{-17}$	$3\cdot0\times10^{-17}$
800A	$0\cdot0693\times10^{10}$	$12\cdot9\times10^{-18}$	$3\cdot3\times10^{-18}$	$1\cdot6\times10^{-17}$	$1\cdot5\times10^{-17}$
850A	$0\cdot276\times10^{10}$	$8\cdot2\times10^{-18}$	$3\cdot2\times10^{-18}$	$1\cdot8\times10^{-17}$	$1\cdot1\times10^{-17}$
900A	$0\cdot326\times10^{10}$	$5\cdot6\times10^{-18}$	$3\cdot1\times10^{-18}$	$2\cdot3\times10^{-17}$	$5\cdot0\times10^{-18}$
950A	$0\cdot0969\times10^{10}$	$3\cdot4\times10^{-18}$	$0\cdot56\times10^{-18}$	$1\cdot3\times10^{-16}$	$6\cdot6\times10^{-17}$
1000A	$0\cdot0260\times10^{10}$	$1\cdot9\times10^{-18}$	$0\cdot00\times10^{-18}$	$2\cdot8\times10^{-17}$	$3\cdot4\times10^{-17}$

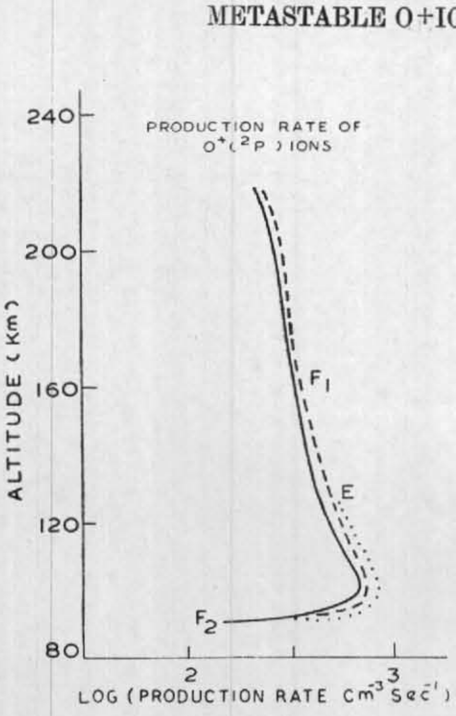

Fig. 5. Production rates of $O^+(^2P)$ ions in the Martian atmosphere

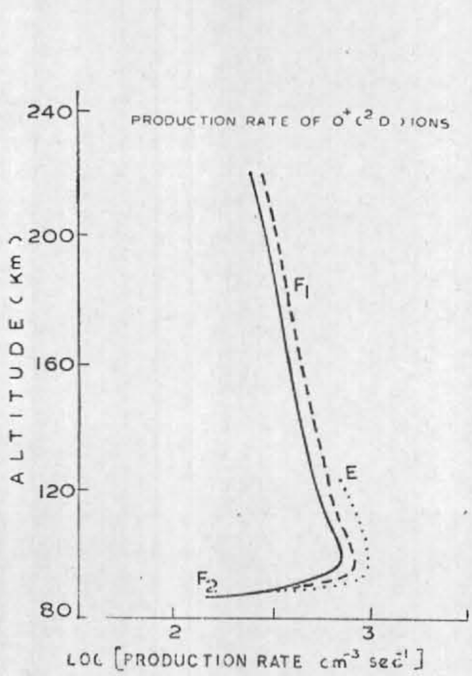

Fig. 6. Production rates of $O^+(^2D)$ ions in the Martian atmosphere

and $O^+(^2D)$ are shown in Figs. 5 and 6 respectively. These figures show that the maximum rates of poduction for both the species occur at about 100 km.

4. Equilibrium concentrations

4.1. $O^+(^2P)$ *ions* — These ions are produced, as mentioned before, by the photo-ionization and also by the spontaneous transitions from excited states of O^+ ions, which are produced when inner electrons are knocked out (Dalgarno *et al.* 1963). However, the later ones can be neglected because of its small cross-sections. $O^+(^2P)$ ions undergo spontaneous transitions to ^2D and ^4S states by —

$$O^+(^2P) \xrightarrow{A_6} O^+(^2D) + P\ (\lambda\ 7330\ A) \tag{6}$$

$$O^+(^2D) \xrightarrow{A_7} O^+(^4S) + P\ (\lambda\ 2440\ A) \tag{7}$$

The transition probability A_6 and A_7 are $0{\cdot}318$/sec and $0{\cdot}080$/sec respectively (Nicholls 1964). These can be de-excited by super-elastic collisions with electrons, *i.e.*,

$$O^+(^2P) + e \xrightarrow{k_8} O^+(^2D) + e \tag{8}$$

$$O^+(^2D) + e \xrightarrow{k_9} O^+(^4S) + e \tag{9}$$

The rate coefficients k_8 and k_9 are 1×10^{-7} cm^3 sec^{-1} and 2×10^{-8} cm^3 sec^{-1} respectively (Seaton and Osterback 1957). Also, these ions will undergo ion-atom interchange with atmospheric molecules, *namely*,

$$O^+ + O_2 \xrightarrow{k_{10}} O_2^+ + O \tag{10}$$

$$O^+ + CO_2 \xrightarrow{k_{11}} O + CO_2^+ \tag{11}$$

Loss of O^+ ions also occurs through the radiative recombination

$$O^+ + e \xrightarrow{k_{12}} O + P \tag{12}$$

However, it may be neglected because, $k_{12} = 4\times10^{-12}$ cm^3 sec^{-1} (Biondi 1964) and electron concentrations over whole of the ionospheric altitudes are small, for it will be an effective loss mechanism.

Hence, if q_1 (O^+) denotes the rate of production of $O^+(^2P)$ due to photo-ionization and n_1 (O^+) its equilibrium concentrations, we have at the equilibrium

$$n_1(O^+) = \frac{q_1(O^+)}{(A_6+A_7)+(k_8+k_9)n(e)+k_{10}\,n(O_2)+k_{11}\,n(CO_2)} \tag{13}$$

4.2. $O^+(^2D)$ *ions* — These ions may be produced by reaction (2), by spontaneous transition (reaction 6) or by super-elastic collision (reaction 8) from ^2P states.

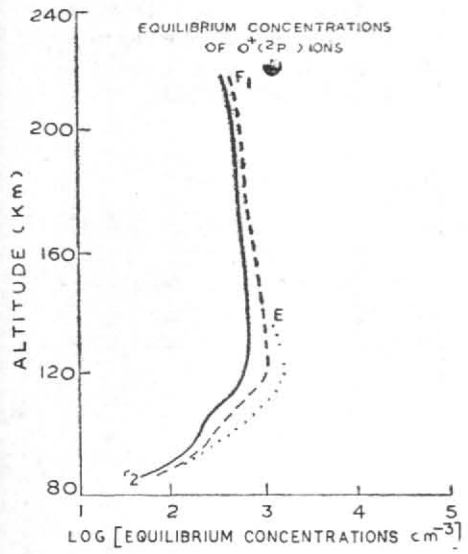

Fig. 7. Equilibrium concentrations of O+(^2P) ions

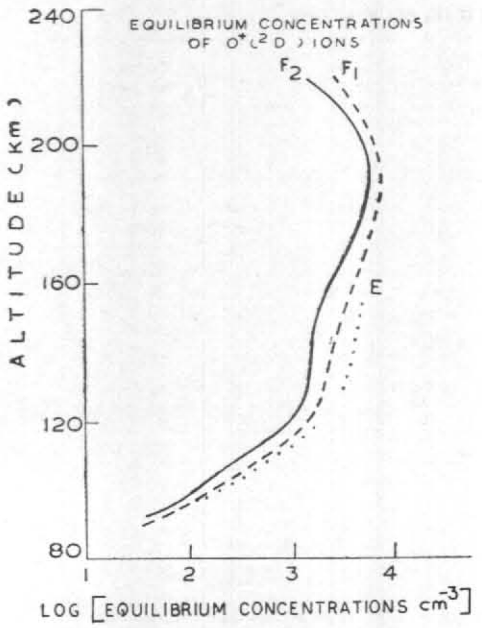

Fig. 8. Equilibrium concentrations of O+(^2D) ions

They are lost to the ground state by super-elastic collisions

$$O^+(^2D) + e \xrightarrow{k_{14}} O^+(^4S) + e \tag{14}$$

(Dalgarno *et al.* 1963), whose rate-coefficient is 3×10^{-8} cm^3 sec^{-1} (Seaton and Osterback 1957) and also through the ion-atom interchange reactions (10) and (11). The loss of $O^+(^2D)$ through spontaneous transitions to the ^4S state is negligble since the corresponding transition probability is $1 \cdot 7 \times 10^{-5}$ sec^{-1} (Nicholls 1964).

Hence, if $q_2(O^+)$ denotes the rate of production of $O^+(^2D)$ by photo-ionization and $n_2(O^+)$ its equilibrium concentration, then at equilibrium,

$$n_2(O^+) = \frac{q_2(O^+) + A_6\, n_1(O^+) n(e) + k_8\, n_1(O^+)\, n(e)}{k_{14}\, n(e) + k_{10}\, n(O_2) + k_{11}\, n(CO_2)} \tag{15}$$

5. Radiation from $O^+(^2P)$

$O^+(^2P)$ ions undergo spontaneous transitions to ^2D state (reaction 6) radiating the multiplet (7318·6 — 7330·7 A), for which the transition probability is equal to 0·318 sec^{-1}. Hence, the volume emission at any altitude z is given by —

$$R_z = n_1(O^+) \times 0 \cdot 318 \tag{16}$$

The integrated intensity of this radiation is calculated in the following way. The altitude region under consideration is divided into thin layers such that the emission rate in each of them is approximately constant. Intensity from each layer is obtained by multiplying mean R_z with the layer thickeness. Summation over all the layers gives the integrated intensity.

6. Results and discussions

Swider (1965) has shown that if $k_{10} = 3 \times 10^{-12}$ cm^3 sec^{-1} for night time earth's atmosphere are assumed, results in agreement with the ionospheric composition determined by rocket-borne spectrometers are obtained. Recently, Ferguson *et al.* (1965) showed that for ions in the ground state $k_{10} = 4 \times 10^{-11}$ cm^3 sec^{-1} at 300°K. Ionospheric calculations indicate that these coefficients are temperture dependent. According to Ghosh (1967), k_{10} should be taken as—

$$k_{10} = 8 \times 10^{-12}\, (1200/T)^{1/2} \text{ cm}^3 \text{ sec}^{-1} \tag{17}$$

where, T is the absolute temperature appropriate to the altitude under consideration.

For k_{11}, Norton *et al.* (1966) found it equal to $1 \cdot 2 \pm 0 \cdot 4 \times 10^{-9}$ cm^3 sec^{-1} at $T = 300$°K. As, no other value of k_{11} are available its temperature study could not be done.

Using Eq (17) and $k_{11} = 1 \cdot 2 \times 10^{-9}$ cm^3 sec^{-1} the equilibrium concentrations of $O^+(^2P)$ and $O^+(^2D)$ ions have been calculated and are shown in Figs. 7 and 8 respectively as a function of altitude.

From relation (16), the integrated intensity R for the transition from $O^+(^2P)$ and $O^+(^2D)$ states is calculated and is tabulated in Table 5. From

TABLE 5

Intensity of the radiation from $O^+(^2P)$ to $O^+(^2D)$

F_2 Model (Rayleighs)	F_1 Model (Rayleighs)	E Model (Rayleighs)
4·60	5·50	7·58

For E model, the intensity R has been calculated from 120 km–0 km altitude because it is difficult to extrapolate the number density of constituent gases above 120 km in the Chamberlain and McElory's (1966) paper. Then from seeing the production rate in F_2 and F_1 model, the intensity (R) for 240-120 km has been assumed and thus total intensity has been found.

this table, it is evident that the intensity for this radiation lies within the limit 4·6 —8·0 Rayleighs. Experimental measurements of this radiation have not been carried out till now. Therefore, it is suggested that the temperature dependence of reaction (11) should be carried out and the experimental measurements of R to be done because the experimental observations on this radiation would help in constructing a better theoretical model.

7. Acknowledgements

I am indebted to Prof. S. N. Ghosh for providing research facilities. I should also thank to Dr. S.K. Jain and Dr. S.K. Gupta for their helpful suggestions. The financial assistance for this work was granted by C.S.I.R., New Delhi, India.

REFERENCES

Biondi, M. A. 1964 *Ann. Geophys.*, **20** p. 34.

Chamberlain, J. W. and McElroy, M. B. 1966 *Science* (USA), **152**, p. 21.

Dalgarno, A. and McElroy, M. B. 1965 *Planet. Space Sci.*, **13**, p. 947.

Dalgarno, A., Stewart, A. L. and Henry, R. J. W. 1964 *Ibid.*, **12**, p.235.

Dalgarno, A., McElroy, M. B. and Moffett, R. J. 1963 *Ibid.*, **11**, p.463.

Donhaue, T. M. 1966 *Science* (USA), **152**, p. 763

Ferguson, E. E. and Fehsenfeld, F. C. 1965 *J. geophys. Res.*, **70**, p. 4323.

Fjeldbo, G. and Eshleman, V. R. 1968 *Planet. Space Sci.*, **16**, p. 1035.

Ghosh, S. N. 1967 *Ionospheric Characteristics from altitude variations of positive ion density*, Scientific Report 05627-9-S, Office of Res. Admin., University of Michigan Ann. Arbor.

Goody, R. 1968 *The Atmosphere of Mars and Venus*, Ed. J. C. Brandt and M. B. McElory, Gordon and Beach, Science Publishers, Inc., New York.

Hinteregger, H. E., Hall, L. A. and Schmidtke, G. 1965 *Space Res.*, **5**, p., 1175.

Mc Elroy, M. B. 1967 *Astrophys. J.*, **150**, p. 1125.

1969 *J. geophys. Res.*, **74**, p.29.

Nicholls, R. W. 1964 *Ann. Geophys.*, **20**, p. 144.

Norton, R. B., Ferguson, E. E., Fehsenfeld, F. C. and Schmeltekopf, A. L. 1966 *Planet. Space Sci.*, **14**, p. 969.

Seaton, J. M. and Osterback, D. E. 1957 *Astrophys. J.*, **125**. p. 66.

Sun, H. and Weissler, G. L. 1955 *J. chem-Phys.*, **23**, p. 1625

Swider, W. 1965 *J. geophys. Res.*, **70**, p. 4859.